Engineering Fracture Mechanics 247 (2021) 107661

Contents lists available at ScienceDirect

Engineering Fracture Mechanics

journal homepage: www.elsevier.com/locate/engfracmech

Technical Note

Characterization of debonding between two different materials with beam like geometries

P. Maimí *, J. Renart, C. Sarrado, E.V. González

AMADE, Mechanical Engineering and Industrial Construction Department, Universitat de Girona, Campus Montilivi s/n, 17003 Girona, Spain

ARTICLE INFO

Keywords:
Composites
Delamination
Interface fracture
Mixed mode fracture
Welded or bonded joints

ABSTRACT

Expressions for the energy release rate and compliance are defined for some asymmetric beam like specimens. The expressions are derived taking into account the Timoshenko beam theory with elastic foundation. The energy release rate is expressed by the applied loads or by a combination of loads and rotation angles, the latter allows to characterize bonded interfaces without taking into account the elastic foundation properties. The condition of stability under displacement controlled test is analysed for typical specimens. The results presented are useful for the characterization of fracture toughness of bimaterial interfaces.

1. Introduction

Stacking layers of different materials allows the definition of shells with tailored properties. This strategy of design is very common in different fields, from packaging, housing, electronics to aeronautics. For example, in aeronautics joining metallic (usually aluminium) and composite layers is usual to improve fatigue and impact response of airplane fuselages [1]. One of the most common form of degradation of these structures is the debonding or delamination of the different layers. Fracture mechanics is the common technique for evaluating the growth of these cracks and the critical fracture energy (G_C) the most important material property required to apply fracture mechanics. Therefore the definition of standard methods to characterize G_C is a need for the safe design of these structures.

To characterize the fracture toughness of composite materials ASTM standards [2–4] can be followed. The scope of these standards only covers symmetric specimens: i.e. the crack defines a symmetric plane and the delamination occurs between the same material. Similar standards are defined to characterize the fracture properties of bonded joints [5]. Analysis through beam theories with or without elastic foundations have been extensively studied for mode I, [6–12] mode II [13–17] and mixed mode fracture [18–23].

The determination of the fracture toughness in interfaces that joins different materials is of great interest because they are more prone to delaminate [24–29]. The objective of this paper is to present the solution of a beam like geometry of bimaterial interfaces considering the Timoshenko beam theory with an elastic foundation. The results presented allow the characterization of fracture properties of bimaterial interfaces subjected to pure mechanical loads. The same model that Williams [10] presented for mode I delamination of symmetric laminates is here extended to mixed mode loading for some particular types of asymmetric laminates.

2. Governing equations based on Timoshenko beam theory and elastic foundations

The geometry of the problem considered is sketched in Fig. 1. The upper U and bottom B arm are made of different material and are partially debonded. At the debonded part of the crack tip (at a coordinate $x = 0^-$) a set of applied loads are known: F_U,

* Corresponding author.
E-mail address: pere.maimi@udg.edu (P. Maimí).

https://doi.org/10.1016/j.engfracmech.2021.107661
Received 19 November 2020; Accepted 2 March 2021
Available online 6 March 2021

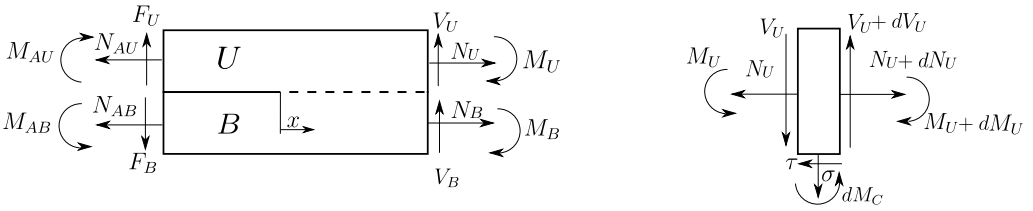

Fig. 1. Beams with applied loads and differential equilibrium of the bonded upper beam.

F_B, M_{AU}, M_{AB}, N_{AU} and N_{AB} that drive the crack growth. In the bonded part the loads can be splitted in N_i, V_i and M_i for $i = U$ and B. The global equilibrium equations are:

$$\begin{aligned} &N_U + N_B = N_{AU} + N_{AB}\ ,\ V_U + V_B = F_B - F_U \text{ and} \\ &M_U + M_B + N_U\tfrac{h_U+h_B}{2} = M_{AB} - M_{AU} + (F_B - F_U)x + N_{AU}\tfrac{h_U+h_B}{2} \end{aligned} \tag{1}$$

the differential equilibrium equations of the upper arm can be expressed as (see Fig. 1)

$$\frac{dN_U}{dx} = \tau \quad , \quad \frac{dV_U}{dx} = \sigma \quad \text{and} \quad V_U = \frac{dM_U}{dx} + \frac{h_U}{2}\frac{dN_U}{dx} - \frac{dM_C}{dx} \tag{2}$$

All the equations of the present paper are normalized with respect to the specimen width.

In the bonded region the stresses at the interface are governed by the elastic foundation constitutive equations:

$$\tau = C_{II} w_{II} \quad , \quad \sigma = C_I w_I \quad \text{and} \quad \frac{dM_C}{dx} = C_\phi \phi_{UB} \tag{3}$$

where w_{II} and w_I are the sliding and opening of the interface and ϕ_{UB} the difference of rotation between upper and bottom arm defined as:

$$w_{II} = u_U - u_B - \frac{h_U}{2}\phi_U - \frac{h_B}{2}\phi_B\ ,\ w_I = w_U - w_B \text{ and } \phi_{UB} = \phi_U - \phi_B \tag{4}$$

The stiffness C_{II} depends on the shear modulus of the arms and C_I on the out-of-plane stiffness. It is usually considered that half of each beam contributes to the stiffness (i.e. for the sliding: $2G_i/h_i$) and the interface behaves like springs in series. Then, for a simple case of two homogeneous arms U and B it is possible to write:

$$\begin{aligned} C_{II} &= 2k_{II}\left(\frac{h_U}{G_U} + \frac{h_B}{G_B}\right)^{-1} \\ C_I &= 2k_I\left(\frac{h_U}{E_{UT}} + \frac{h_B}{E_{BT}}\right)^{-1} \\ C_\phi &= \frac{k_\phi}{2}\left(\frac{1}{h_U G_U} + \frac{1}{h_B G_B}\right)^{-1} \end{aligned} \tag{5}$$

where G_i and E_{iT} are the shear and out-of-plane modulus of each beam, respectively. k_I and k_{II} are fitting parameters usually taken as 1 or fitted by numerical models. The bending stiffness C_ϕ has a more complex interpretation, as argued by Olsson [30] the effect of the bending stiffness is redundant with the consideration of Timoshenko beam theory because it is similar to the shear stiffness of the beam. The constant k_ϕ in Eq. (5) is usually defined as 5/6. Following the work of Williams [10], which is the foundation of the standardized method to characterize the DCB specimen, here the problem is solved by considering C_ϕ.

According to Timoshenko beam theory the constitutive equations that defines the relation between the loads (N_i, M_i and V_i) and the kinematics (u_i, ϕ_i and w_i) of each arm ($i = U$ and B) reads:

$$\begin{bmatrix} \frac{du_i}{dx} \\ \frac{d\phi_i}{dx} \end{bmatrix} = \begin{bmatrix} a_i & b_i \\ b_i & d_i \end{bmatrix} \begin{bmatrix} N_i \\ M_i \end{bmatrix} \quad \text{and} \quad \frac{dw_i}{dx} + \phi_i = k_i V_i \tag{6}$$

where k_i is the shear compliance of each arm, defined as $k_i = (k_s G_i h_i)^{-1}$, where k_s is a factor usually considered as 5/6.

From the defined hypothesis, constitutive and equilibrium equations, it is possible to obtain the following differential equations with respect to variables w_I and w_{II} as defined in Appendix:

$$\frac{d^4 w_I}{dx^4} - \left(\beta_0 C_I - \beta_1 C_\phi\right)\frac{d^2 w_I}{dx^2} - \beta_1 C_I\left(1 + C_\phi\beta_0\right) w_I + \alpha_1 C_{II}\frac{dw_{II}}{dx} = 0 \tag{7a}$$

$$\frac{d^3 w_{II}}{dx^3} - C_{II}\left(\alpha_2 - \alpha_1\frac{h_U}{2}\right)\frac{dw_{II}}{dx} - \alpha_1\left(C_I\left(1 + C_\phi\beta_0\right) w_I - C_\phi\frac{d^2 w_I}{dx^2}\right) = 0 \tag{7b}$$

It is important to note that both variables are coupled by the parameter α_1. Bennati et al. [26], Liu et al. [27] and Qiao and Wang [31] presented the solution of this equations for $C_\phi = 0$.

At this point it is of interest to define some constants that will be used throughout the paper:

$$\begin{aligned}
\alpha_1 &= b_U + b_B - \tfrac{d_U h_U - d_B h_B}{2} \\
\alpha_2 &= a_U + a_B + b_B h_B + h_U \tfrac{b_B - b_U}{2} + d_B h_B \tfrac{h_B + h_U}{4} \\
\alpha_3 &= 2b_B + h_B d_B \\
\beta_0 &= k_U + k_B \\
\beta_1 &= -(d_U + d_B) \\
\beta_2 &= -\left(b_U + b_B + d_B \tfrac{h_U + h_B}{2}\right)
\end{aligned} \tag{8}$$

The loads at the upper arm can be computed by means of Eq. (2):

$$N_U = C_{II} \int w_{II} dx \tag{9a}$$

$$V_U = C_I \int w_I dx \tag{9b}$$

$$M_U = \int \left(V_U + C_\phi \phi_{UB}\right) dx - \frac{h_U}{2} N_U \tag{9c}$$

where from Eq. (A.3):

$$\phi_{UB} = \beta_0 V_U - \frac{dw_I}{dx} - k_B (F_B - F_U) \tag{10}$$

At some distance from the crack front (at large values of x) the following conditions can be considered: $dw_I/dx = dw_{II}/dx = d\phi_{UB}/dx = 0$. Taking into account the constitutive and equilibrium Eqs. (A.1), (A.3) and (A.8) the following loads at upper arm are obtained:

$$V_U^R = \frac{k_B}{\beta_0}(F_B - F_U) + \frac{\phi_{UB}^R}{\beta_0} \tag{11a}$$

$$\begin{bmatrix} M_U^R \\ N_U^R \end{bmatrix} = \begin{bmatrix} \beta_1 & \beta_2 \\ \alpha_1 & \alpha_2 \end{bmatrix}^{-1} \begin{bmatrix} -d_B \left(F_B - F_U\right) x - d\phi_{UB}^R \\ \frac{\alpha_3}{2} \left(F_B - F_U\right) x + dw_{II}^R \end{bmatrix} \tag{11b}$$

where ϕ_{UB}^R is the difference of rotation angle between upper and bottom arms, $d\phi_{UB}^R$ and dw_{II}^R are defined by Eqs. (A.2) and (A.9) of Appendix.

3. The mixed mode energy release rate of asymmetric beams

The determination of the fracture toughness of symmetric specimens is well defined and standardized. In this case a symmetric loading results in pure mode I and antisymmetric loading in pure mode II. For asymmetric specimens there are several ways to determine the mixed mode, it is worth highlighting the following two methods:

- Local partition
  The local solution is defined by solving the complete stress field of the problem. Some solutions are presented by several authors in [24,32–37]. Davidson et al. [35] presented a fitting equation for wide applicability. The local solution is the correct solution of linear elastic fracture mechanics.
- Williams partition
  According to Williams [38] the pure mode II is defined by loading cases that produce the same curvature of both arms at the crack tip ($x = 0$):

  $$\frac{d\phi_U}{dx} = \frac{d\phi_B}{dx}$$

  This allows the decomposition of general case by considering orthogonality of partitioning. This condition is equivalent to define pure mode I as the obtained by a standard DCB specimen.

There are several other partition methods, see for example [28,39–44], a critical comparison of these methods can be found in Maimíet al. [45]. In general, the different ways to determine the mode mixity lead to different results when the specimen is asymmetric. A question arises of which is the correct way to determine the mode I or mode II contributions in the energy release rate for asymmetric specimens.

Of special interest are the experimental tests performed by Kinloch et al. [46] and Ducept et al. [47]. These authors characterized an interface following the standard methods with symmetric specimens and latter compared the results with asymmetric specimens defined by means of different arm thickness. The results of both tests seem contradictory because according to Kinloch et al. [46] the Williams method is more appropriate while for Ducept et al. [47] the local method leads to the correct decomposition. As

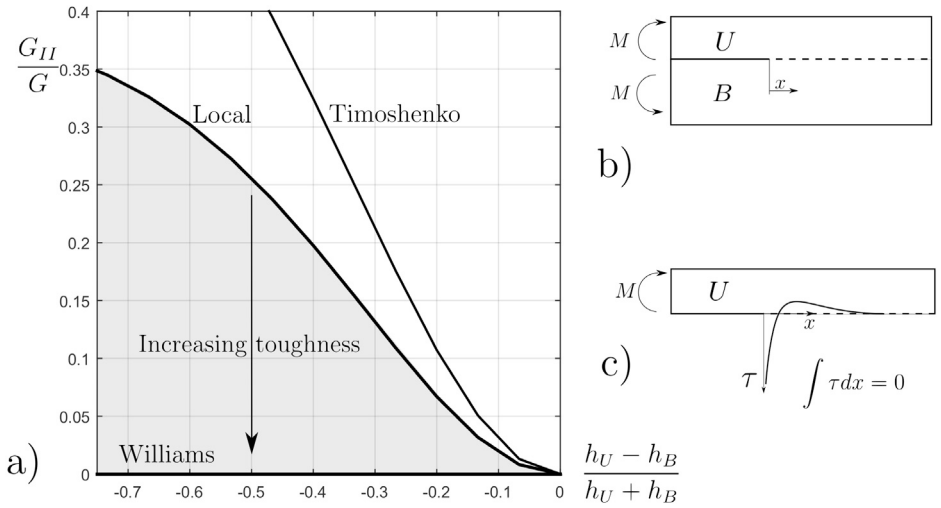

Fig. 2. (a) Mixed mode of beam like specimens of the same material and different arm thickness, (b) geometry with loadings and (c) shear stress at the bonded interface.

noted by several authors [36,47–49] the size of the K-dominant zone is very small in beam-like geometries, usually smaller than the failure process zone. Numerical results presented by Conroy et al. [50] and Maimíet al. [45] confirm with asymmetric specimens and cohesive models that for brittle interfaces which develop a very small failure process zone, the local method is appropriate, on the other case for very tough interfaces, with large failure process zone, the Williams [38] method results in the correct decomposition. These two partition methods seem to be the two extreme cases, whereas in the intermediate cases the actual mixed mode is at some point between these two limiting theories.

In Fig. 2.a the partition of energy release rate according to local (for isotropic materials), Williams and Timoshenko beam (without elastic foundation) for a specimen with the same material at bottom and upper arms but with different thickness is shown. The loading case considered is a symmetric bending as shown in Fig. 2.b. It must be pointed out, that Timoshenko differs significantly from the local method in the case of stiff interfaces, if the elastic foundation is taken into account the Timoshenko can be very close to the local method if the appropriate interface stiffness is used. This is proven by the results presented by Bennati et al. [26] with $k_I = 3.45$ and $k_{II} = 8.1$ and by Valvo [28] with $k_I = k_{II} = 5$, both cases with $C_\phi = 0$ where results of mixed mode are quite similar to the local solution. For symmetric specimens ($h_U = h_B$) all partition criteria deal with pure mode I loading. In Fig. 2.c the elastic shear stress at the interface for $h_U \neq h_B$ is sketched, at crack tip the shear stress is not null and produces a mixed mode loading as predicted by local (and Timoshenko) theories. On the other hand, by taking into account the global equilibrium $\int \tau dx = 0$, then at some distance the shear stress changes its sign and tends to zero afterwards, if the cohesive non linear zone is large enough the shear stresses are watered down and crack grows in pure mode I according to Williams (or global) partition. This example intuitively explains the dependence of the mixed mode on the length of the cohesive zone that in turns depends on the fracture toughness [45,46,50].

Taking into account the differential equation (7) it can be easily observed that both equations are coupled by means of the parameter α_1. If $\alpha_1 \neq 0$ it is possible to determine a set of loadings that produce $w_{II} = 0$ at crack tip ($x = 0$) but not along the interface, then pure mode I will be obtained only for very brittle interfaces. The same can be argued with a pure mode II loading. On the other hand, if $\alpha_1 = 0$ both equations are uncoupled, and a symmetric loading cause $w_{II} = 0$ across all the interface length and pure mode I is guaranteed independently of the cohesive zone length.

Since the mixed mode of the general case ($\alpha_1 \neq 0$) depends on the fracture toughness which is the material property that can be measured, the mode mixity of these specimens cannot be predicted in advance and has to be recalculated a posteriori by some method. It can be done by reproducing the test with numerical methods [45] or by applying the semi-analytical method proposed by Conroy et al. [50] that depends on an estimate of the cohesive zone length. If possible, the optimum solution is to design specimens in which $\alpha_1 = 0$ [45,51,52], then:

$$d_U h_U - 2b_U = d_B h_B + 2b_B \tag{12}$$

in this case, the two governing Eqs. (7) are uncoupled and it is possible to find a load case that produce $w_I = 0$ for all x, that will result in pure mode II and a load case that produce $w_{II} = 0$ for all x that will result in pure mode I.

4. General solution of the uncoupled case

If the parameter $\alpha_1 = 0$, the governing Eqs. (7) can be simplified as:

$$\frac{d^4 w_I}{dx^4} - 2c_2 \frac{d^2 w_I}{dx^2} + c_0^2 w_I = 0 \tag{13a}$$

$$\frac{d^2 w_{II}}{dx^2} - C_{II}\alpha_2 w_{II} + \frac{\alpha_3}{2}\left(F_B - F_U\right) = 0 \tag{13b}$$

where

$$2c_2 = \beta_0 C_I - \beta_1 C_\phi \quad \text{and} \quad c_0^2 = -\beta_1 C_I \left(1 + C_\phi \beta_0\right) \tag{14}$$

Since they are uncoupled, the linear differential equations can be solved independently to get $w_I(x)$ and $w_{II}(x)$.

4.1. Crack sliding: w_{II}

The solution of Eq. (13b) is

$$w_{II} = w_{II}^R + \left(w_{II0} - w_{II}^R\right)\exp\left(-x\sqrt{C_{II}\alpha_2}\right) \tag{15}$$

where $w_{II}^R = \alpha_3\left(F_B - F_U\right)/\left(2\alpha_2 C_{II}\right)$. The normal load is defined by means of Eq. (9a) with an integration constant defined by the boundary condition expressed by Eq. (11b). w_{II0} can be determined by considering that $N_U = N_{AU}$ at $x = 0$:

$$w_{II0} = \frac{\alpha_3}{2}\Delta_{II}\left(M_{II}^* + \Delta_{II}\left(F_B - F_U\right)\right) \tag{16}$$

where

$$M_{II}^* = M_{AB} - M_{AU} + \frac{2\left(a_B^* N_{AB} - a_U^* N_{AU}\right)}{\alpha_3} \quad \text{and} \quad \Delta_{II} = \left(\alpha_2 C_{II}\right)^{-1/2} \tag{17}$$

where $a_B^* = a_B + \frac{h_B}{2} b_B$ and $a_U^* = a_U - \frac{h_U}{2} b_U$

4.2. Crack opening: w_I

The solution of Eq. (13a) depends on the roots of the characteristic polynomial: $\xi^2 - 2c_2\xi + c_0^2 = 0$, according to:

$$\begin{aligned}
&c_2 > c_0, \quad \xi_{1,2}^2 = c_2 \pm \sqrt{c_2^2 - c_0^2} && w_I = \tfrac{w_{I0}\xi_2 + w_{I1}}{\xi_2 - \xi_1} e^{-x\xi_1} - \tfrac{w_{I0}\xi_1 + w_{I1}}{\xi_2 - \xi_1} e^{-x\xi_2} \\
&c_2 < c_0, \quad 2\xi_{1,2}^2 = c_0 \pm c_2 && w_I = e^{-x\xi_1}\left(w_{I0}\cos(\xi_2 x) + \tfrac{w_{I0}\xi_1 + w_{I1}}{\xi_2}\sin(\xi_2 x)\right) \\
&c_2 = c_0, \quad \xi^2 = c_0 = c_2 && w_I = e^{-x\xi}(w_{I0} + (w_{I0}\xi + w_{I1})x)
\end{aligned}$$

The shear (V_U) and moment (M_U) at the upper arm can be determined by means of Eqs. (9a) and (9c). At large x it is necessary to enforce the limit solution expressed by Eq. (11). From this it is also possible to define:

$$\phi_{UB}^R = \kappa_{UB}^R\left(F_B - F_U\right) \quad \text{where} \quad \kappa_{UB}^R = \frac{d_U k_B - k_U d_B}{\beta_1\left(1 + \beta_0 C_\phi\right)} \tag{18}$$

The shear and moment at $x = 0$ are defined by the boundary conditions F_U and M_{AU}. This allows to define the constants w_{I0} and w_{I1}, which represent the crack opening and its derivative with respect to x at crack tip, and the angle ϕ_{UB0} defined by means of Eq. (10).

$$\begin{aligned}
w_{I0} &= \frac{\beta_1}{c_0 - \beta_1 C_\phi}\left(-\frac{c_0\sqrt{2}\sqrt{c_0 + c_2}}{\beta_1 C_I} F_I^* + M_I^*\right) \\
w_{I1} &= \frac{\beta_1}{c_0 - \beta_1 C_\phi}\left(c_0\frac{c_0 + C_I\beta_0}{\beta_1 C_I} F_I^* - \sqrt{2}\sqrt{c_0 + c_2} M_I^*\right) \\
\phi_{UB0} &= \frac{\beta_1}{c_0 - \beta_1 C_\phi}\left(F_I^* + \sqrt{2}\sqrt{c_0 + c_2} M_I^*\right) + \phi_{UB}^R
\end{aligned} \tag{19}$$

where

$$\begin{aligned}
M_I^* &= \frac{1}{\beta_1}\left(d_U M_{AU} + d_B M_{AB} - b_U N_{AU} + b_B N_{AB}\right) \\
F_I^* &= \frac{\left(d_B - k_B C_\phi \beta_1\right)F_B + \left(d_U - k_U C_\phi \beta_1\right)F_U}{\beta_1\left(1 + \beta_0 C_\phi\right)}
\end{aligned} \tag{20}$$

4.3. Energy release rate

The energy release rate in mode I and mode II can be determined by means of the expressions:

$$G_I = \frac{1}{2}\left(C_I w_{I0}^2 + C_\phi \phi_{UB0}^2\right) \tag{21a}$$

$$G_{II} = \frac{1}{2} C_{II} w_{II0}^2 \tag{21b}$$

The total energy release rate: $G = G_I + G_{II}$.

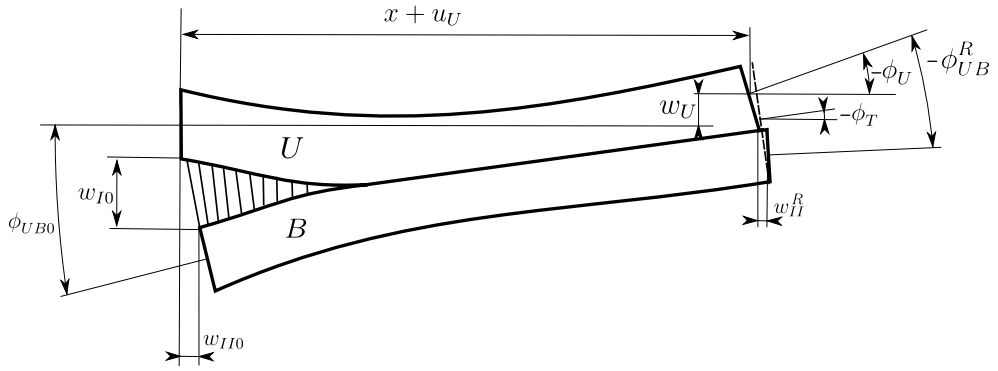

Fig. 3. Beams with applied loads and differential equilibrium of the bonded upper beam.

4.4. Displacements

The displacements can be determined by means of Eq. (6) taking into account the loads of Eq. (9) (see Fig. 3):

$$u_U = \int (a_U N_U + b_U M_U) dx \approx U_{U0} + U_{U1} x + U_{U2} x^2 \tag{22a}$$

$$\phi_U = \int (b_U N_U + d_U M_U) dx \approx \Phi_{U0} + \Phi_{U1} x + \Phi_{U2} x^2 \tag{22b}$$

$$w_U = \int (k_U V_U - \phi_U) dx \approx W_{U0} + W_{U1} x + W_{U2} x^2 + W_{U3} x^3 \tag{22c}$$

for large enough values of x a polynomial approximation allows to describe the displacements (when a term related to $\exp(-\xi_i x)$ is negligible). By means of Eq. (9) and the solution of w_I and w_{II} it is possible to determine the parameters:

$$U_{U0} = \frac{-a^*_U \alpha_3}{2\alpha_2 \sqrt{C_{II}\alpha_2}} M^*_{II} + \frac{b_U}{c_0 - C_\phi \beta_1} F^*_I + \frac{b_U \sqrt{2}\sqrt{c_0 + c_2}}{c_0 - C_\phi \beta_1} M^*_I$$
$$U_{U1} = -\frac{b_U}{\beta_1} d\phi^R_{UB} + \frac{a^*_U}{\alpha_2} dw^R_{II}$$
$$U_{U2} = -\frac{1}{2}\left(\frac{b_U d_B}{\beta_1} - \frac{a^*_U \alpha_3}{2\alpha_2}\right)(F_B - F_U)$$

$$\Phi_{U0} = \frac{\alpha_3^2}{4\alpha_2 \sqrt{C_{II}\alpha_2}} M^*_{II} + \frac{d_U}{c_0 - C_\phi \beta_1} F^*_I + \frac{d_U \sqrt{2}\sqrt{c_0 + c_2}}{c_0 - C_\phi \beta_1} M^*_I$$
$$\Phi_{U1} = -\frac{d_U}{\beta_1} d\phi^R_{UB} - \frac{\alpha_3}{2\alpha_2} dw^R_{II}$$
$$\Phi_{U2} = -\frac{1}{2}\left(\frac{d_U d_B}{\beta_1} + \frac{\alpha_3^2}{4\alpha_2}\right)(F_B - F_U)$$

$$W_{U0} = \frac{\alpha_3^2}{4 C_{II} \alpha_2^2} M^*_{II} + \frac{\sqrt{2}\sqrt{c_0 + c_2}(d_U - k_U C_\phi \beta_1)}{c_0 (c_0 - C_\phi \beta_1)} F^* + \frac{d_U c_0 + C_I (d_U k_B - d_B k_U)}{c_0 (c_0 - C_\phi \beta_1)} M^*$$
$$W_{U1} = \frac{k_U}{\beta_0}\left(\phi^R_{UB} + k_B (F_B - F_U)\right) - \Phi_{U0}$$
$$W_{U2} = -\frac{\Phi_{U1}}{2}$$
$$W_{U3} = -\frac{\Phi_{U2}}{3}$$

The vertical displacement of the bonded beam is equal to the displacement of the upper beam $w_T = w_U$, the rotation can be defined as: $\phi_T = \phi_U - \phi^R_{UB} k_U / \beta_0$.

4.5. Stability of the test under displacement control

In a test with a dominant mode II component it is common to have an unstable crack propagation even under displacement control. The definition of an appropriate initial notch length is important to avoid this undesirable response.

Most of the tests used to determine the fracture toughness are performed by applying a single controlled displacement (u) and the corresponding load is recorded (F), both related to the specimen compliance as: $u = C(a)F$, where a is the crack length. Taking into account the only source of work in the system is due to u, the total ERR can be defined as:

$$G = \frac{u^2}{2C^2}\frac{dC}{da} \tag{23}$$

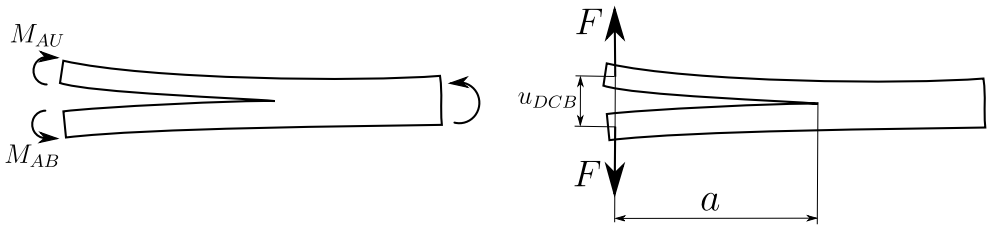

Fig. 4. Specimen under bending loads and DCB specimen.

the crack will increase if the fracture mechanics is fulfilled: $G = G_C$, being G_C the critical fracture energy of the interface. The stability under displacement controlled test can be defined by the derivative of Eq. (23) [53,54]: $dG/da < dG_C/da \approx 0$. This results into the condition

$$C\frac{d^2C}{da^2} < 2\left(\frac{dC}{da}\right)^2 \tag{24}$$

A first approximation of the compliance that results from Euler beam theory without foundation stiffness is of the form:

$$C \approx C_a a^3 + C_L L^3 \tag{25}$$

where L is the specimen length and a the crack length. Then the stability under displacement control is obtained if the following condition holds:

$$\frac{a}{L} > \left(\frac{C_L}{2C_a}\right)^{\frac{1}{3}} \tag{26}$$

It must be pointed out that Eq. (26) is usually a conservative limit since the foundation stiffness and the formation of a cohesive zone tends to decrease the initial stable notch length [55,56].

5. Solution of the uncoupled case for typical specimens

In this section the energy release rate and compliance functions for some typical loading cases are presented and discussed for uncoupled specimens ($\alpha_1 = 0$).

5.1. Specimens under bending loads

In Fig. 4, a specimen with applied bending loads is shown, the crack growth is governed by two independent applied bending moments: M_{AU} and M_{AB}. The mode I and mode II ERR is defined by Eq. (21) as:

$$G_I = \frac{\left(d_U M_{AU} + d_B M_{AB}\right)^2}{2(d_U + d_B)} \quad \text{and} \quad G_{II} = \frac{\alpha_3^2}{8\alpha_2}\left(M_{AB} - M_{AU}\right)^2 \tag{27}$$

where $d_U M_{AU} + d_B M_{AB} \geq 0$ to avoid contact between the arms.

The application of bending loads have some special advantages against the typical application of forces; the ERR does not depend on the crack length, as a consequence Eqs. (27) are valid for large displacements and if the ratio of applied loads is constant the mixed mode ERR is also constant, the crack grows in self-similar regime and the response is also valid for large cohesive zones. Furthermore the shear and out-of-plane elastic properties do not influence the ERR. In spite of the previously mentioned advantages the apparatus required to apply moments is more complex that the ones that apply forces and it is not widely used yet [57,58]. Finally, the pure mode I is obtained when the moments at both arms are equal $M_{AU} = M_{AB}$, and pure mode II when $d_U M_{AU} + d_B M_{AB} = 0$ if the condition $\alpha_1 = 0$ holds.

5.2. Double Cantilever Beam (DCB)

For the DCB specimen the applied load F produces at crack tip: $F_U = F_B = F$ and $M_{AU} = M_{AB} = Fa$. According to Eq. (16) $w_{I10} = 0$ and a DCB specimen produces pure mode I loading. The displacement at applied loads can be determined as:

$$u_{DCB} = \frac{d_U + d_B}{3} F a^3 + \beta_0 F a + \phi_{UB0} a + w_{I0}$$

Taking into account equation (19) it is possible to define the compliance as:

$$C_{DCB} = \frac{u_{DCB}}{F} = \frac{d_U + d_B}{3}\left(a^3 + 3\Delta_I a^2 + 3\Delta_{IL}^2 a + \Delta_{IC}^3\right) \tag{28}$$

where

$$\Delta_I = \frac{\sqrt{2}\sqrt{c_0 + c_2}}{c_0 - \beta_1 C_\phi} \quad , \quad \Delta_{IL}^2 = \frac{2}{c_0 - \beta_1 C_\phi} - \frac{\beta_0}{\beta_1} \quad \text{and} \quad \Delta_{IC}^3 = \frac{-3c_0}{\beta_1 C_I}\Delta_I \tag{29}$$

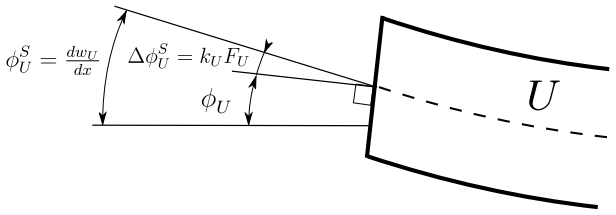

Fig. 5. Relation between the angles of the beam.

The energy release rate can be determined by means of Eq. (21a) or by the compliance method:

$$G_I = \frac{d_U + d_B}{2} F^2 (a^2 + 2\Delta_I a + \Delta_{IL}^2) \tag{30}$$

The term Δ_I is the most important and it is quite common to simplify expressions (28) and (30) as:

$$C_{DCB} \approx \frac{d_U + d_B}{3} \left(a + \Delta_I\right)^3 \tag{31a}$$

$$G_I \approx \frac{d_U + d_B}{2} (a + \Delta_I)^2 F^2 \tag{31b}$$

If $C_\phi = 0$ the following equality holds: $\Delta_I = \Delta_{IL}^2$ and the ERR of Eq. (31) is exact, not the compliance because $\Delta_I \neq \Delta_{IC}$. The same solution presented here has been published for symmetric laminates in Kanninen [6] and Williams [10]. For the case of $C_\phi = 0$ the results are equivalent to the solution presented by Kondo [12] and if $\beta_0 = 0$ (Euler beam) by Kanninen [59] and Ozdil and Carlsson [9].

For orthotropic monomaterial joints, with principal material directions oriented in the crack direction, the parameter Δ_I results

$$\Delta_I = h\sqrt{\frac{E}{18k_sG}} \sqrt{3 - \frac{EE_Tk_I\frac{k_\phi+k_s}{k_s} + 3(k_\phi - k_s)G\left(Gk_\phi + 2\sqrt{EE_Tk_I\frac{k_\phi+2k_s}{3k_s}}\right)}{\left(Gk_\phi + \sqrt{EE_Tk_I\frac{k_\phi+2k_s}{3k_s}}\right)^2}}$$

where E and E_T are the in-plane and out-of-plane Young's modulus respectively, and G the shear modulus. This result is equal to the obtained by Williams [10] with $k_\phi = k_s$ and $k_I = 1$:

$$\Delta_I = h\sqrt{\frac{E}{18k_sG}} \sqrt{3 - \frac{2EE_T}{\left(k_sG + \sqrt{EE_T}\right)^2}}$$

Williams [10] proposed a fitting for Δ_I that reproduce a set of numerical results:

$$\Delta_I = h\sqrt{\frac{E}{11G}} \sqrt{3 - \frac{2EE_T}{\left(50G/59 + \sqrt{EE_T}\right)^2}} \tag{32}$$

this result is obtained by considering $k_s = k_\phi = 11/18$ and $k_I = 0.52$.

It must be pointed out that the Δ_I, usually used with Eq. (31), is adjusted by means of finite element method to obtain precise enough results. This procedure is still more complex for specimens considered in this paper where the upper and bottom arms are of different materials.

By means of Rice [60] and Cherepanov [61] J-integral, Paris and Paris [62] showed that for a symmetric DCB specimen the following relation holds: $J = F\phi_{DCB}^S$, where ϕ_{DCB}^S is the rotated angle at load application point, determined as the derivative of out-of-plane displacement. By considering the angles shown in Fig. 5: $\phi_{DCB}^S = \phi_{DCB} + \Delta\phi_{DCB}^S$, where $\phi_{DCB} = (d_U + d_B)Fa/2 + \phi_{UB0}$ and $\Delta\phi_{DCB}^S = \beta_0 F$, Eq. (30) can be expressed as:

$$G_I = F\phi_{DCB}^S \tag{33}$$

ϕ_{DCB}^S can be measured by the difference of angles of two inclinometers bonded at the load application points of the upper and bottom beam surfaces. This is a remarkable result because allows the determination of the fracture energy without considering the elastic properties of the materials, specially those related with the out-of-plane direction.

5.3. Fixed mixed mode ratio specimens

Single Cantilever Beam (SCB) and Single Leg Bending (SLB) specimens allow a mixed mode ERR by pulling a single arm as shown in Fig. 6, for symmetric laminates the mixed mode is approximately $G_{II}/G \approx 3/7$ for large enough crack lengths (a).

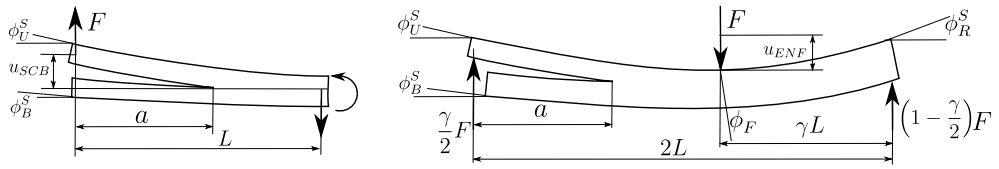

Fig. 6. Single Cantilever Beam (SCB) and Single Leg Bending (SLB) specimens.

5.3.1. Single Cantilever Beam (SCB)

By considering that $M_{AU} = Fa$ and $F_U = F$ as the only applied loads at crack tip, the mode I and II ERR are defined as:

$$G_I = \frac{d_U^2}{d_U + d_B}\frac{F^2}{2}\left(a^2 + 2\Delta_I a + \xi\Delta_{IL}^2\right) + k_U C_\phi \kappa_{UB}^R \frac{F^2}{2} \tag{34a}$$

$$G_{II} = F^2 \frac{\alpha_3^2}{8\alpha_2}\left(a + \Delta_{II}\right)^2 \tag{34b}$$

where $\xi = (d_U - \beta_1 k_U C_\phi)/(d_U(1 + \beta_0 C_\phi))$.

The displacement at loading point can be computed by the expression: $u_{SCB} = \frac{d_U}{3}Fa^3 + k_U Fa - w_T - \phi_T L$, where w_T and ϕ_T are the displacement and angle of the bonded part defined in Section 4.4. The compliance is defined as:

$$\begin{aligned} C_{SCB} = \; & \frac{d_U^2}{3(d_U+d_B)}\left(a^3 + 3\Delta_I a^2 + 3\xi\Delta_{IL}^2 a + \xi^2\Delta_{IC}^3\right) + \\ & + \frac{\alpha_3^2}{12\alpha_2}\left(a + \Delta_{II}\right)^3 + d_T\frac{L^3}{3} + k_T L + k_U C_\phi \kappa_{UB}^R a - \frac{\alpha_3^2}{12\alpha_2}\Delta_{II}^3 \end{aligned} \tag{35}$$

where

$$d_T = \frac{d_U d_B}{d_U + d_B} - \frac{\alpha_3^2}{4\alpha_2} \quad \text{and} \quad k_T = \frac{k_U k_B}{k_U + k_B} \tag{36}$$

are the bending and shear compliances of the bonded part of the beam, respectively.

The ERR of the SCB can also be expressed taking into account the rotation of the surface of the beam at applied point according to the expression:

$$G = F\phi_U^S - \left(\frac{d_T}{2}L^2 + k_{SCB}\right)F^2 \tag{37}$$

where $\phi_U^S = d_U Fa^2/2 - \phi_T + Fk_U$ is the rotation angle at the surface where the load is applied as shown in Fig. 6. The only significant term in the parenthesis is the term $d_T L^2$. The shear coefficient is defined as

$$k_{SCB} = k_T - \frac{\xi d_U}{2\beta_1}(k_U + k_{UB}^R) - \frac{\alpha_3^2\Delta_{II}^2}{8\alpha_2} - \frac{C_\phi}{2}\left(k_{UB}^R\right)^2$$

The first two terms are related with the shear stiffness of the beam and the last two to the remaining rotation and shear displacement w_{II}^R and ϕ_{UB}^R (see Fig. 3).

The mode I ERR can also be defined taking into account the rotation angles as:

$$G_I = F\frac{d_U}{d_U + d_B}\left(\phi_U^S - \phi_B^S\right) - \left(\frac{\xi d_U^2\beta_0}{\beta_1^2} - k_U C_\phi \kappa_{UB}^R\right)\frac{F^2}{2} \tag{38}$$

where $\phi_B^S = -\phi_{UB0} - \phi_T$ is the rotation angle at the surface of the bottom arm. The mode II ERR can be obtained taking into account Eqs. (37) and (38): $G_{II} = G - G_I$.

Neglecting the last term in Eq. (34a) the mixed mode $B = G_{II}/G$ is defined as

$$B \approx \frac{\alpha_3^2(d_U+d_B)}{\alpha_3^2(d_U+d_B)+4\alpha_2 d_U^2 R_a^2} \quad \text{where} \quad R_a = \frac{\sqrt{a^2+2\Delta_I a+\xi\Delta_{IL}^2}}{a+\Delta_{II}} \tag{39}$$

where for common specimens $R_a \approx 1$. It must be pointed out that for asymmetric specimens two different mixed mode ratio can be obtained by turning the specimen upside down.

Under displacement control the stability condition is defined by Eq. (24), taking into account that a^3 is the most important term a simplification of Eq. (26) can be applied result in:

$$\frac{a}{L} > \left(\frac{d_T}{2(d_U - d_T)}\right)^{\frac{1}{3}} \tag{40}$$

For a specimen with two homogeneous arms of longitudinal Young modulus, E_U and E_B that holds the condition $E_U h_U^2 = E_B h_B^2$, the mixed mode and the stability condition can be approximated as:

$$B = \frac{G_{II}}{G} \approx \frac{3}{3+4\sqrt{E_U/E_B}} \quad \text{and} \quad \frac{a}{L} > 0.415 \left(\frac{7}{3+4\sqrt{E_U/E_B}} \right)^{\frac{1}{3}} \tag{41}$$

5.3.2. Single Leg Bending (SLB)

The SLB specimen is shown in Fig. 6, commonly defined with $\gamma = 1$. The mode I and II energy release rate are expressed as:

$$G_I = \frac{d_U^2}{d_U + d_B} \frac{\gamma^2 F^2}{8} \left(a^2 + 2\Delta_I a + \xi \Delta_{IL}^2 \right) + k_U C_\phi \kappa_{UB}^R \frac{\gamma^2 F^2}{8} \tag{42a}$$

$$G_{II} = \gamma^2 F^2 \frac{\alpha_3^2}{32\alpha_2} \left(a + \Delta_{II} \right)^2 \tag{42b}$$

The mixed mode is the same as for the SCB specimen and is defined by Eq. (39).

The displacement, taking into account the left part of the specimen, is defined as:

$$u_{SLB} = \frac{d_U}{3} \frac{\gamma F}{2} a^3 + k_U \frac{\gamma F}{2} a - w_T - (\phi_T + \phi_F) L (2 - \gamma) \tag{43}$$

where ϕ_F is the rotation angle at load application point (as defined in Fig. 6). The displacement can also be expressed taking into account the right part of the beam as:

$$u_{SLB} = \left(d_T \frac{\gamma^3 L^3}{3} + k_T L \gamma \right) \left(1 - \frac{\gamma}{2} \right) F + \gamma L \phi_F \tag{44}$$

By solving the previous two equations the displacement and rotation at loading point can be defined, from here the compliance is:

$$\begin{aligned} C_{SLB} = \; & \frac{\gamma^2 d_U^2}{12(d_U + d_B)} \left(a^3 + 3\Delta_I a^2 + 3\xi \Delta_{IL}^2 a + \xi^2 \Delta_{IC}^3 \right) + \frac{\gamma^2 \alpha_3^2}{48\alpha_2} \left(a + \Delta_{II} \right)^3 \\ & + d_T \frac{(2-\gamma)^2 \gamma^2}{6} L^3 + k_T \frac{(2-\gamma)\gamma}{2} L + \frac{k_U C_\phi \kappa_{UB}^R \gamma^2}{4} a - \frac{\gamma^2 \alpha_3^2}{48\alpha_2} \Delta_{II}^3 \end{aligned} \tag{45}$$

The ERR can also be expressed with respect to some rotation angles defined in Fig. 6:

$$G = \left(\gamma \left(\phi_U^S + \phi_F \right) - (2 - \gamma) \left(\phi_R^S - \phi_F \right) \right) \frac{F}{2} + k_{SLB} F^2 \tag{46}$$

where the term shear term k_{SLB} is usually negligible and is defined as:

$$k_{SLB} = (1 - \gamma) k_T + \frac{\gamma^2}{8} \left(\frac{\xi d_U}{\beta_1} (k_U + k_{UB}^R) + \frac{\alpha_3^2 \Delta_{II}^2}{4\alpha_2} + C_\phi (k_{UB}^R)^2 \right)$$

The mode I ERR can be expressed as:

$$G_I = \frac{\gamma}{2} F \frac{d_U}{d_U + d_B} \left(\phi_U^S - \phi_B^S \right) - \left(\frac{\xi d_U^2 \beta_0}{\beta_1^2} - k_U C_\phi \kappa_{UB}^R \right) \frac{\gamma^2 F^2}{8} \tag{47}$$

where ϕ_B^S is the rotation angle of the bottom arm of the specimen as shown in Fig. 6.

An approximation of the stability condition for the test under displacement control is defined by Eq. (26):

$$\frac{a}{L} > \left(\frac{(2-\gamma)^2 d_T}{d_U - d_T} \right)^{\frac{1}{3}} \tag{48}$$

For two homogeneous materials it is simplified as:

$$\frac{a}{L} > 0.523 \left(\frac{7(2-\gamma)^2}{3 + 4\sqrt{E_U/E_B}} \right)^{\frac{1}{3}} \tag{49}$$

5.4. Mode II specimens

End-Loaded Split (ELS) and End-Notched Flexure (ENF) tests shown in Fig. 7 are typical configurations to measure the mode II fracture energy [14,17], both are standardized for symmetric specimens by ISO [63] and ASTM [4], respectively.

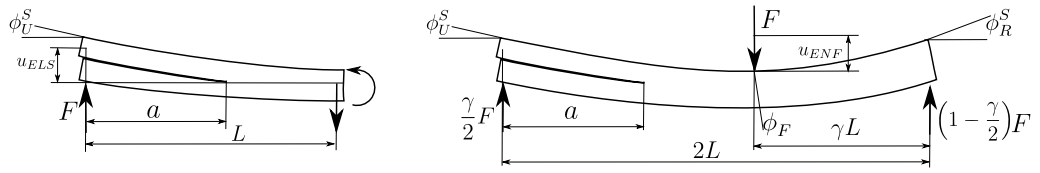

Fig. 7. End-Loaded Split (ELS) and End-Notched Flexure (ENF) tests.

5.4.1. End-Loaded Split (ELS)

By global equilibrium the loads in the bottom arm are defined as: $F_B = F_U - F$, $M_{AB} = M_{AU} - Fa$ and $N_B = N_U = 0$, since no shear stress are assumed to be present in the unbonded region. By means of this global conditions of equilibrium and Eqs. (16) and (21b), the mode II energy release rate can be defined:

$$G_{II} = \frac{F^2}{8}\frac{\alpha_3^2}{\alpha_2}\left(a + \Delta_{II}\right)^2 \tag{50}$$

In ELS and ENF specimens the load is applied in the bottom arm and is transferred to the upper arm by the contact of both arms, for symmetric laminates the contact load is limited in a narrow region near the applied load, numerical results shows a relatively small contribution of friction to energy dissipation [53,64–67]. For asymmetric specimens the contact load is not limited to a small region at load line due to the non-proportionality of bending and shear stiffness of both arms. The equilibrium equation of the unbounded upper arm is defined by considering a null crack opening ($w_I = 0$), by means of the derivative of Eq. (A.3), introducing equation (A.1) and taking into account $N_U = 0$ and $V_U = dM_U/dx$. The following differential equation is defined:

$$\frac{d^2 w_I}{dx^2} = \beta_0 \frac{d^2 M_U}{dx^2} + \beta_1 M_U - d_B F x = 0 \tag{51}$$

where $x = 0$ is the position of the loading point. Note that Eq. (51) is obtained by considering a stiff contact between the arms. The solution of this differential equation is:

$$M_U = \frac{-F}{d_U + d_B}\left[d_B x + \frac{C_\phi \beta_1 \kappa_{UB}^R}{1 + (1 + C_\phi \beta_0)^{-1/2}}\sqrt{\frac{-\beta_0}{\beta_1}}\frac{\sinh\left(x\sqrt{\frac{-\beta_1}{\beta_0}}\right)}{\sinh\left(a\sqrt{\frac{-\beta_1}{\beta_0}}\right)}\right]$$

The condition of $w_{I1} = 0$ for stiff contact ($C_I \to \infty$) at crack tip is imposed. The contact stress in the interface is determined by the second derivative of the bending moment and is expected to be negative: $\sigma = d^2 M_U/dx^2 \le 0$, this condition holds if $\kappa_{UB}^R \le 0$:

$$k_B d_U \ge k_U d_B \tag{52}$$

this usually corresponds with the thicker bottom arm.

The specimen compliance can be computed by taking into account the displacement defined in Eq. (22):

$$C_{ELS} = \frac{\alpha_3^2}{12\alpha_2}\left(a + \Delta_{II}\right)^3 + d_T\frac{L^3}{3} + k_T L - \frac{\alpha_3^2}{12\alpha_2}\Delta_{II}^3 + C_{ELS}^{(a)} a - C_{ELS}^{(c)} \tag{53}$$

where

$$C_{ELS}^{(a)} = C_\phi (k_{UB}^R)^2\left(1 + C_\phi \beta_0\right) \quad \text{and} \quad C_{ELS}^{(c)} = \frac{(C_\phi k_{UB}^R)^2 \beta_0}{1+(1+\beta_0 C_\phi)^{-1/2}}\sqrt{\frac{-\beta_0}{\beta_1}} \tag{54}$$

It must be pointed out that the ERR computed by the compliance method is not exactly the defined by Eq. (50) because there is a term related with the rotation at crack tip and the stiffness C_ϕ: $G_I = C_{ELS}^{(a)} F^2/2$. This ERR is zero for symmetric laminates and negligible in practical cases.

The ERR can also be defined by considering the rotation angle at load point as shown in Fig. 7:

$$G = \phi_U^S F - \left(\frac{d_T}{2}L^2 + k_{ELS}\right)F^2 \tag{55}$$

where k_{ELS} is negligible in practical cases and is expressed as:

$$k_{ELS} = \frac{-k_U d_B}{\beta_1} - k_{UB}^R\left(\frac{k_U}{\beta_0} - \frac{C_\phi d_U \beta_0}{\beta_1}\right) - \frac{C_{ELS}^{(a)}}{2} - \frac{\alpha_3^2 \Delta_{II}^2}{8\alpha_2}$$

The required length to obtain a stable test response under controlled displacement can be approximated:

$$\frac{a}{L} > \left(\frac{2\alpha_2 d_T}{\alpha_3^2}\right)^{1/3}$$

For homogeneous material this condition is reduced to: $a/L > 0.55$.

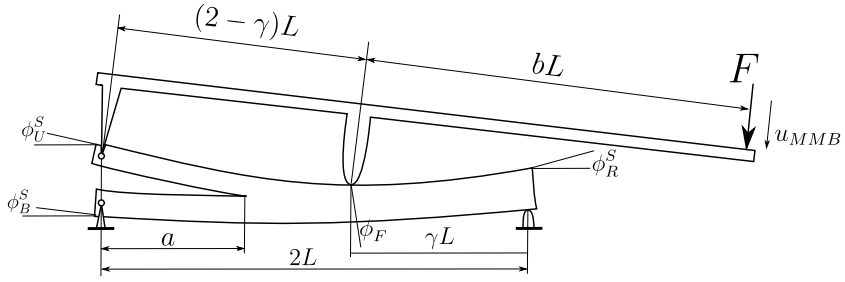

Fig. 8. Mixed Mode Bending (MMB) test.

5.4.2. End-Notched Flexure (ENF)

The geometry of the ENF specimen is sketched in Fig. 7. The standard specimen is defined with $\gamma = 1$ [4]. Following the same arguments shown in the previous subsection for the ELS specimen, the ENF energy release rate is:

$$G_{II} = \frac{\gamma^2 F^2}{32}\frac{\alpha_3^2}{\alpha_2}\left(a + \Delta_{II}\right)^2 \tag{56}$$

To enforce contact between the two arms and minimize the mode I contribution the condition of Eq. (52) holds also for ENF specimen.

The compliance of the ENF specimen can be obtained by taking into account equation (22):

$$C_{ENF} = \frac{\gamma^2\alpha_3^2}{48\alpha_2}\left(a + \Delta_{II}\right)^3 + \frac{d_T(2-\gamma)^2\gamma^2}{6}L^3 + \frac{k_T(2-\gamma)\gamma}{2}L - \frac{\gamma^2\alpha_3^2}{48\alpha_2}\Delta_{II}^3 + \frac{\gamma^2 C_{ELS}^{(a)} a}{4} \tag{57}$$

The length Δ_{II} is defined in Eq. (17), for a laminate with the same material at both arms: $\Delta_{II} = h\sqrt{E/(8Gk_{II})}$. The presented form of Δ_{II} is the same obtained by Chatterjee [15] with $k_{II} = 7.39$ and also by Wang and Qiao [16] with $k_{II} = 7.5$ who find the parameter k_{II} by fitting finite element results. On the other hand, this relation differs significantly from the empirical expression determined by Wang and Williams [13]: $\Delta_{II} = 0.43\Delta_I$ where Δ_I is the empirical equation (32) defined by $k_s = k_\phi = 11/18$ and $k_I = 0.52$. To obtain the same results with the proposed expression than the common definition of Wang and Williams [13] it is required to define k_{II} as:

$$k_{II} = \frac{63}{8}\left(3 - \frac{2EE_T}{\left(50G/59 + \sqrt{EE_T}\right)^2}\right)^{-1}$$

where k_{II} is not constant and it can change between 2.65 to 7.87 by decreasing the shear modulus. This equation depends on the out-of-plane modulus (E_T) contrary to the results of Chatterjee [15] and Wang and Qiao [16], the present solution and also the numerical results presented by Wang and Williams [13].

As in the previous cases the difficulty to define Δ_{II} can be overcomed by means of the measurements of the rotation angles defined in Fig. 7:

$$G = \left(\gamma\left(\phi_U^S + \phi_F\right) - (2-\gamma)\left(\phi_R^S - \phi_F\right)\right)\frac{F}{2} + k_{ENF}F^2 \tag{58}$$

where

$$k_{ENF} = (1-\gamma)k_T + \frac{\gamma^2}{8}\left(k_T + \frac{k_U d_B}{\beta_1} + k_{UB}^R\left(\frac{k_U}{\beta_0} - \frac{C_\phi d_U \beta_0}{\beta_1}\right) + \frac{\alpha_3^2\Delta_{II}^2}{4\alpha_2}\right)$$

The ENF specimen is known to be unstable in most of the cases, the condition of stable crack growth is defined as:

$$\frac{a}{L} > \left(\frac{4\alpha_2 d_T(2-\gamma)^2}{\alpha_3^2}\right)^{\frac{1}{3}} \tag{59}$$

For beams with two homogeneous materials it results in $a/L > 0.69(2-\gamma)^{1/3}$ [53], note that the stability condition does not depend on the ratio E_U/E_B.

5.5. Mixed Mode Bending (MMB) test

The mixed mode bending test sketched in Fig. 8 allows the determination of different relation between mode I and mode II by changing the length ratio b [18,19,21–23]. This test is ASTM standardized [3] for symmetric laminates with $\gamma = 1$.

The applied loads at crack tip (see Fig. 1) are $M_{AU} = F_U a$, $M_{ABU} = F_B a$, $F_U = bF/(2-\gamma)$ and $F_B = (b-\gamma)F/2$. It is of interest to define

$$m_I = \frac{1}{\beta_1}\left(d_B \frac{b-\gamma}{2} + d_U \frac{b}{2-\gamma}\right) \quad \text{and} \quad m_{II} = \frac{b-\gamma}{2} - \frac{b}{2-\gamma} \tag{60}$$

The mode I and II ERR can be expressed as:

$$G_I = \frac{(d_U + d_B)F^2}{2}\left(m_I^2\left(a^2 + 2\Delta_I a + \Delta_{IL}^2\right) + \Delta_\phi^2\right) \tag{61a}$$

$$G_{II} = F^2 \frac{m_{II}^2 \alpha_3^2}{8\alpha_2}\left(a + \Delta_{II}\right)^2 \tag{61b}$$

where

$$\Delta_\phi^2 = \frac{C_\phi m_{II} \kappa_{UB}^R}{d_U + d_B}\left(\kappa_{UB}^R(1 + \beta_0 C_\phi)m_{II} + \left(\beta_0 - \beta_1 \Delta_{IL}^2\right) m_I\right)$$

The compliance of the MMB specimen is defined by the expression:

$$\begin{aligned} C_{MMB} = {} & \frac{m_{II}^2 \alpha_3^2}{12\alpha_2}\left(a + \Delta_{II}\right)^3 + \frac{m_I^2(d_U + d_B)}{3}\left(a^3 + 3\Delta_I a^2 + 3\Delta_{IL}^2 a + \Delta_{IC}^3\right) \\ & + d_T \frac{2m_{II}^2(2-\gamma)^2}{3} L^3 + k_T \frac{2m_{II}^2(2-\gamma)}{\gamma} L + (d_U + d_B)\Delta_\phi^2 a + C_{MMB}^{(c)} \end{aligned} \tag{62}$$

where

$$C_{MMB}^{(c)} = \frac{m_{II}\Delta_{IC}^3}{3}\left(m_I d_B + \frac{C_\phi \kappa_{UB}^R b}{2-\gamma}\right) - \frac{m_{II}^2 \alpha_3^2}{12\alpha_2}\Delta_{II}^3$$

To avoid the determination of the foundation properties of the material it is possible to measure the rotation angles of Fig. 8, in this case the ERR can be expressed as:

$$G = \left(b\frac{\phi_U^S + \phi_F}{2-\gamma} - (b-\gamma)\frac{\phi_B^S + \phi_F}{2} - (2 + b - \gamma)\frac{\phi_R^S - \phi_F}{2}\right)F + k_{MMB}F^2 \tag{63}$$

where

$$\begin{aligned} k_{MMB} = {} & \left(\frac{2+(2-m_I)(b-\gamma)}{2} + \frac{bm_{II}}{2-\gamma} - \frac{m_{II}d_U(d_B m_{II} + \beta_1 m_I)}{\beta_1^2}\right)k_T + \frac{m_{II}^2\alpha_3^2\Delta_{II}^2}{8\alpha_2} \\ & - \frac{\beta_0 m_I^2}{2} + m_{II}^2 k_{UB}^R\left(\frac{2d_U}{\beta_1} - \frac{k_{UB}^R\left(C_\phi^2\beta_0^2 + 5C_\phi\beta_0 + 4\right)}{2\beta_0}\right) - \frac{m_I m_{II}(d_U k_B^2 - d_B k_U^2)}{\beta_0\beta_1} \end{aligned}$$

as in the previous cases the contribution of k_{MMB} is insignificant for long specimens. The mode I ERR can be determined as:

$$G_I = -m_I\left(\phi_U^S - \phi_B^S\right)F - \left(m_I^2\beta_0 - m_{II}^2 C_\phi (k_{UB}^R)^2(1 + \beta_0 C_\phi)\right)\frac{F^2}{2} \tag{64}$$

Neglecting the small term Δ_ϕ in G_I of Eq. (61a) the mixed mode is defined as:

$$B \approx \frac{m_{II}^2\alpha_3^2}{m_{II}^2\alpha_3^2 + 4m_I^2\alpha_2(d_U + d_B)R_a^2} \quad \text{where} \quad R_a = \frac{\sqrt{a^2 + 2\Delta_I a + \Delta_{IL}^2}}{a + \Delta_{II}} \tag{65}$$

The mixed mode depends on the length of the arm bL, it is of special interest to know the value of b to obtain a desired mixed mode ratio B. Neglecting the small term Δ_ϕ:

$$b \approx \gamma(\gamma - 2)\frac{\alpha_3^2\beta_1\gamma R_b + 4\alpha_2 d_B(d_B\gamma + 2\beta_1)R_a^2 + 4R_a\beta_1\alpha_3\sqrt{-R_b\beta_1\alpha_2}}{4R_a^2\alpha_2(2\beta_1 + d_B\gamma)^2 + \alpha_3^2\beta_1\gamma^2 R_b}$$

where $R_b = (1 - B)/B$.

The required crack length to have a stable propagation can be approximated as:

$$\frac{a}{L} > \left(\frac{4B(2-\gamma)^2 d_T \alpha_2}{\alpha_3^2}\right)^{\frac{1}{3}} \tag{66}$$

6. Conclusions

In the present contribution the required equations to characterize the interface between different materials are presented based on Timoshenko beam theory with elastic foundation. The solution is presented for beams that hold the following relation: $d_U h_U - 2b_U = d_B h_B + 2b_B$, this relation appears to be mandatory to obtain a consistent mixed mode; i.e. an independent mixed mode with respect to the fracture toughness.

Some useful expressions of the compliance and energy release of common specimens are defined. The energy release rate is defined by the applied loads and also taking into account some rotation angles, the latter requires the measurement of rotations by means of inclinometers but are almost independent of the foundation parameters that usually are fitted with numerical models. Finally, the conditions of stable test under displacement control are defined. The results presented are useful to characterize the interface fracture properties of bonded materials with beam-like geometry specimens.

Declaration of competing interest

The authors declare that they have no known competing financial interests or personal relationships that could have appeared to influence the work reported in this paper.

Acknowledgement

This work has been partially funded by the Spanish Government through the Ministerio de Economía y Competitividad, under contract RTI2018-097880-B-I00.

Appendix. Differential equations

From the derivative of ϕ_{UB} in (4) and introducing bending constitutive Eqs. (6) and equilibrium Eqs. (1)

$$\frac{d\phi_{UB}}{dx} = -\beta_1 M_U - \beta_2 N_U + d_B\left(F_U - F_B\right)x - d\phi^R_{UB} \tag{A.1}$$

where

$$d\phi^R_{UB} = d_B\left(M_{AB} - M_{AU} + N_{AU}\frac{h_U + h_B}{2}\right) + b_B(N_{AU} + N_{AB}) \tag{A.2}$$

From the derivative of w_I in (4) and introducing bending constitutive Eqs. (6) and equilibrium Eqs. (1)

$$\frac{dw_I}{dx} = \beta_0 V_U - \phi_{UB} - k_B(F_B - F_U) \tag{A.3}$$

By derivating twice and introducing equation (A.1)

$$\frac{d^3 w_I}{dx^3} = \beta_0\frac{d^2 V_U}{dx^2} + \beta_1\frac{dM_U}{dx} + \beta_2\frac{dN_U}{dx} - d_B\left(F_U - F_B\right) \tag{A.4}$$

By means of bending equilibrium of Eq. (1)

$$\frac{d^3 w_I}{dx^3} = \beta_0\frac{d^2 V_U}{dx^2} + \beta_1\left(V_U - \frac{h_U}{2}\frac{dN_U}{dx} + \frac{dM_C}{dx}\right) + \beta_2\frac{dN_U}{dx} - d_B\left(F_U - F_B\right) \tag{A.5}$$

derivating again and with load equilibrium of Eq. (1) and the foundation Eqs. (3)

$$\frac{d^4 w_I}{dx^4} = \beta_0 C_I\frac{d^2 w_I}{dx^2} + \beta_1\left(C_I w_I - \frac{h_U}{2}C_{II}\frac{dw_{II}}{dx} + C_\phi\frac{d\phi_{UB}}{dx}\right) + \beta_2 C_{II}\frac{dw_{II}}{dx} \tag{A.6}$$

ϕ_{UB} can be defined by means of Eq. (A.3)

$$\frac{d^4 w_I}{dx^4} = \left(\beta_0 C_I - \beta_1 C_\phi\right)\frac{d^2 w_I}{dx^2} + \beta_1 C_I\left(1 + \beta_0 C_\phi\right)w_I + C_{II}\left(\beta_2 - \beta_1\frac{h_U}{2}\right)\frac{dw_{II}}{dx} \tag{A.7}$$

To obtain the other differential equation it is necessary to derive w_{II} in Eq. (4):

$$\frac{dw_{II}}{dx} = \alpha_2 N_U + \alpha_1 M_U - \frac{\alpha_3}{2}\left(F_B - F_U\right)x - dw^R_{II} \tag{A.8}$$

where

$$dw^R_{II} = \frac{\alpha_3}{2}\left(M_{AB} - M_{AU} + N_{AU}\frac{h_U + h_B}{2}\right) + \left(a_B + \frac{h_B}{2}b_B\right)(N_{AU} + N_{AB}) \tag{A.9}$$

It is possible to determine its derivative and substitute the shear elastic foundation constitutive equation:

$$\frac{d^2 w_{II}}{dx^2} = \alpha_2 C_{II} w_{II} + \alpha_1\frac{dM_U}{dx} - \frac{\alpha_3}{2}\left(F_B - F_U\right) \tag{A.10}$$

To eliminate the bending moment M_U we can proceed as after equation (A.4)

$$\frac{d^3 w_{II}}{dx^3} = C_{II}\left(\alpha_2 - \alpha_1\frac{h_U}{2}\right)\frac{dw_{II}}{dx} + \alpha_1\left(C_I\left(1 + C_\phi\beta_0\right)w_I - C_\phi\frac{d^2 w_I}{dx^2}\right) \tag{A.11}$$

References

[1] Vogelesang LB, Roebroeks GHJJ. EP Patent 0312151: Laminate of metal sheets and continuous glass filaments-reinforced synthetic material. AKZO NV; 1991.
[2] ASTM D 5528 – 01. Standard test method for mode I interlaminar fracture toughness of unidirectional. Amer Soc Test Mater 2004;03:1–12.
[3] D6671M A. Standard test method for mixed mode I-Mode II interlaminar fracture toughness of unidirectional fiber reinforced polymer matrix composites. ASTM Int 2006;15. http://dx.doi.org/10.1520/D6671.
[4] ASTM D7905/D7905M-14. Standard test method for determination of the mode II interlaminar fracture toughness of unidirectional fiber-reinforced polymer matrix composites. Amer Soc Test Mater 2014;15.03:1–18. http://dx.doi.org/10.1520/D7905.
[5] ISO 25217:2009. Adhesives — Determination of the mode I adhesive fracture energy of structural adhesive joints using double cantilever beam and tapered double cantilever beam specimens. International Organization for Standardization; 2009.
[6] Kanninen MF. A dynamic analysis of unstable crack propagation and arrest in the DCB test specimen. Int J Fract 1974;10(3):415–30.
[7] Kanninen MF. An augmented double cantilever beam model for studying crack propagation and arrest. Int J Fract 1973;9(1):83–91.
[8] Whitney JM. Stress analysis of the double cantilever beam specimen. Compos Sci Technol 1985;23(3):201–19. http://dx.doi.org/10.1016/0266-3538(85)90018-1.
[9] Ozdil F, Carlsson LA. Beam analysis of angle-ply laminate DCB specimens. Compos Sci Technol 1999;59(2):305–15. http://dx.doi.org/10.1016/S0266-3538(98)00069-4.
[10] Williams JG. End corrections for orthotropic DCB specimens. Compos Sci Technol 1989;35(4):367–76. http://dx.doi.org/10.1016/0266-3538(89)90058-4.
[11] Olsson R. A simplified improved beam analysis of the DCB specimen. Compos Sci Technol 1992;43(4):329–38. http://dx.doi.org/10.1016/0266-3538(92)90056-9.
[12] Kondo K. Analysis of double cantilever beam specimen. Adv Compos Mater 1995;4(4):355–66. http://dx.doi.org/10.1163/156855195X00203.
[13] Wang Y, Williams JG. Corrections for mode II fracture toughness specimens of composite materials. Compos Sci Technol 1992;43(43:3):251–6.
[14] Davies P, Sims GD, Blackman BRK, Brunner AJ, Kageyama K, Hojo M, et al. Comparison of test configurations for determination of mode II interlaminar fracture test programme. Plast Rubber Compos 1999;2–7.
[15] Chatterjee SN. Analysis of test specimens for interlaminar mode II fracture toughness, part 1. Elastic laminates. J Compos Mater 1991;25:470–93. http://dx.doi.org/10.1177/002199839102500501.
[16] Wang J, Qiao P. Novel beam analysis of end notched flexure specimen for mode-II fracture. Eng Fract Mech 2004;71(2):219–31. http://dx.doi.org/10.1016/S0013-7944(03)00096-1.
[17] Blackman BRK, Brunner AJ, Williams JG. Mode II fracture testing of composites: a new look at an old problem. Eng Fract Mech 2006;73:2443–55. http://dx.doi.org/10.1016/j.engfracmech.2006.05.022.
[18] Reeder JR, Crews Jr JR. A mixed-mode bending method for delamination testing. AIAA J 1990;28(7):1270–6.
[19] Reeder JR. An evaluation of mixed-mode delamination failure criteria, Nasa Technical Memorandum. 1992.
[20] Davies P, Blackman BRK, Brunner AJ. Standard test methods for delamination resistance of composite materials: Current status. Appl Compos Mater 1998;5:345–64.
[21] Pereira AB, de Morais AB. Mixed mode I + II interlaminar fracture of glass/epoxy multidirectional laminates – Part 2: Experiments. Compos Sci Technol 2006;66:1896–902. http://dx.doi.org/10.1016/j.compscitech.2006.04.008.
[22] Bennati S, Fisicaro P, Valvo PS. An enhanced beam-theory model of the mixed-mode bending (MMB) test — Part I: Literature review and mechanical model. Meccanica 2013;48:463. http://dx.doi.org/10.1007/s11012-013-9697-8, (erratum).
[23] Bennati S, Fisicaro P, Valvo PS. An enhanced beam-theory model of the mixed-mode bending (MMB) test — Part II: Applications and results. Meccanica 2013;48:465–84. http://dx.doi.org/10.1007/s11012-012-9682-7.
[24] Xiao F, Hui CY, Kramer EJ. Analysis of a mixed mode fracture specimen: the asymmetric double cantilever beam. J Mater Sci 1993;28(20):5620–9. http://dx.doi.org/10.1007/BF00367838.
[25] Balendran B. On the double cantilever beam specimen for mode-I interface delamination. J Appl Mech 1994;61(2):471–3. http://dx.doi.org/10.1115/1.2901470.
[26] Bennati S, Colleluori M, Corigliano D, Valvo PS. An enhanced beam-theory model of the asymmetric double cantilever beam (ADCB) test for composite laminates. Compos Sci Technol 2009;69(11–12):1735–45. http://dx.doi.org/10.1016/j.compscitech.2009.01.019.
[27] Liu Z, Huang Y, Yin Z, Bennati S, Valvo PS. A general solution for the two-dimensional stress analysis of balanced and unbalanced adhesively bonded joints. Int J Adhes Adhes 2014;54:112–23, arXiv:13960/t7pn90p77.
[28] Valvo PS. On the calculation of energy release rate and mode mixity in delaminated laminated beams. Eng Fract Mech 2016;165:114–39. http://dx.doi.org/10.1016/j.engfracmech.2016.08.010.
[29] Delbariani-Nejad A, Malakouti M, Farrokhabadi A. Reliability analysis of metal-composite adhesive joints under debonding modes I, II, and I/II using the results of experimental and FEM analyses. Fatigue Fract Eng Mater Struct 2019;42(12):2644–62. http://dx.doi.org/10.1111/ffe.13078.
[30] Olsson R. On improper foundation models for the DCB specimen. In: 16th international conference on composite materials. 2007. p. 1–6.
[31] Qiao P, Wang J. Mechanics and fracture of crack tip deformable bi-material interface. Int J Solids Struct 2004;41(26):7423–44. http://dx.doi.org/10.1016/j.ijsolstr.2004.06.006.
[32] Suo Z, Hutchinson JW. Interface crack between two elastic layers. Int J Fract 1990;43(5):1–18. http://dx.doi.org/10.1007/Bf00018123.
[33] Beuth JL. Separation of crack extension modes in orthotropic delamination models. Int J Fract 1996;77(4):305–21. http://dx.doi.org/10.1007/BF00036249.
[34] Schapery RA, Davidson BD. Prediction of energy release rate for mixed-mode delamination using classical plate theory. Appl Mech Rev 1990;43(5S):S281.
[35] Davidson BD, Hu H, Schapery RA. An analytical crack-tip element for layered elastic structures. J Appl Mech 1995;62(June 1995):294–305. http://dx.doi.org/10.1115/1.2895931.
[36] Davidson BD, Gharibian SJ, Yu L. Evaluation of energy release rate-based approaches for predicting delamination growth in laminated composites. Int J Fract 2000;105(4):343–65. http://dx.doi.org/10.1023/A:1007647226760.
[37] Davidson BD, Yu L, Hu H. Determination of energy release rate and mode mix in three-dimensional layered structures using plate theory. Int J Fract 2000;105(1):81–104. http://dx.doi.org/10.1023/A:1007672131026.
[38] Williams JG. On the calculation of energy release rates for cracked laminates. Int J Fract 1988;36(2):101–19. http://dx.doi.org/10.1007/BF00017790, URL http://link.springer.com/10.1007/BF00017790.
[39] Luo Q, Tong L. Analytic formulas of energy release rates for delamination using a global-local method. Int J Solids Struct 2012;49(23–24):3335–44.
[40] Wang S, Harvey CM. Mixed mode partition theories for one dimensional fracture. Eng Fract Mech 2012;79:329–52. http://dx.doi.org/10.1016/j.engfracmech.2011.11.013.
[41] Harvey CM, Wang S. Mixed-mode partition theories for one-dimensional delamination in laminated composite beams. Eng Fract Mech 2012;96:737–59.
[42] Bruno D, Greco F. Mixed mode delamination in plates: a refined approach. Int J Solids Struct 2001;38:9149–77.
[43] Wang J, Qiao P. Interface crack between two shear deformable elastic layers. J Mech Phys Solids 2004;52(4):891–905. http://dx.doi.org/10.1016/S0022-5096(03)00121-2.

[44] Tsokanas P, Loutas T. Hygrothermal effect on the strain energy release rates and mode mixity of asymmetric delaminations in generally layered beams. Eng Fract Mech 2019;214(March):390–409. http://dx.doi.org/10.1016/j.engfracmech.2019.03.006.
[45] Maimí P, Gascons N, Ripoll L, Llobet J. Mixed mode delamination of asymmetric beam-like geometries with cohesive stresses. Int J Solids Struct 2018;155:36–46.
[46] Kinloch AJ, Wang Y, Williams JG, Yayla P. The mixed-mode delamination of fibre composite materials. Compos Sci Technol 1993;47(3):225–37. http://dx.doi.org/10.1016/0266-3538(93)90031-B.
[47] Ducept F, Gamby D, Davies P. A mixed-mode failure criterion derived from test on symmetric and asymmetric specimens. Compos Sci Technol 1999;59:609–19. http://dx.doi.org/10.1016/S0266-3538(98)00105-5.
[48] Charalambides M, Kinloch AJ, Wang Y, Williams JG. On the analysis of mixed-mode failure. Int J Fract 1992;54(3):269–91. http://dx.doi.org/10.1007/BF00035361.
[49] Becker T, McNaney J, Cannon R, Ritchie RO. Limitations on the use of the mixed-mode delaminating beam test specimen: Effects of the size of the region of K-dominance. Mech Mater 1997;25(4):291–308. http://dx.doi.org/10.1016/S0167-6636(97)00010-0.
[50] Conroy M, Kinloch AJ, Williams JG, Ivankovic A. Mixed mode partitioning of beam-like geometries: A damage dependent solution. Eng Fract Mech 2015;149(1):351–67. http://dx.doi.org/10.1016/j.engfracmech.2015.06.061.
[51] Ouyang Z, Li G. Nonlinear interface shear fracture of end notched flexure specimens. Int J Solids Struct 2009;46(13):2659–68. http://dx.doi.org/10.1016/j.ijsolstr.2009.02.011.
[52] Ouyang Z, Ji G, Li G. On approximately realizing and characterizing pure mode-I interface fracture between bonded dissimilar materials. J Appl Mech 2011;78(3):031020. http://dx.doi.org/10.1115/1.4003366.
[53] Carlsson LA, Gillespie JW, Pipes RB. On the analysis and design of the end notched flexure (ENF) specimen for mode II testing. J Compos Mater 1986;20(6):594–604.
[54] Ortega A, Maimí P, González EV, Ripoll L. Compact tension specimen for orthotropic materials. Composites A 2014;63:85–93. http://dx.doi.org/10.1016/j.compositesa.2014.04.012.
[55] Alfredsson KS. On the instantaneous energy release rate of the end-notch flexure adhesive joint specimen. Int J Solids Struct 2004;41:4787–807. http://dx.doi.org/10.1016/j.ijsolstr.2004.03.008.
[56] Pérez-Galmés M, Renart J, Sarrado C, Brunner AJ, Rodríguez-Bellido A. Towards a consensus on mode II adhesive fracture testing: Experimental study. Theor Appl Fract Mech 2018;98(October):210–9. http://dx.doi.org/10.1016/j.tafmec.2018.09.014.
[57] Plausinis D, Spelt JK. Application of a new constant g load-jig to creep crack growth in adhesive joints. Int. J. A 1995;15(4):225–32.
[58] Sørensen BF, Jørgensen K, Jacobsen TK, Østergaard RC. DCB-Specimen loaded with uneven bending moments. Int J Fract 2006;141(1–2):163–76. http://dx.doi.org/10.1007/s10704-006-0071-x.
[59] Kanninen MF. An augmented double cantilever beam model for studying crack propagation and arrest. Int J Fract 1973;9(1):83–92.
[60] Rice JR. A path independent integral and approximate analysis of strain concentration by notches and cracks. J Appl Mech 1968;35(2):379.
[61] Cherepanov GP. Crack propagation in continuous media. J Appl Math Mech 1967;31(3):476–88. http://dx.doi.org/10.1016/0021-8928(67)90034-2.
[62] Paris AJ, Paris PC. Instantaneous evaluation of J and C*. Int J Fract 1988;1:8–10.
[63] ISO15114:2014. Fibre-reinforced plastic composites — Determination of the mode II fracture resistance for unidirectionally reinforced materials using the calibrated end-loaded split (C-ELS) test and an effective crack length approach. International Organization for Standardization; 2014.
[64] Gillespie JW, Carlsson LA, Pipes RB. Finite element analysis of the end notched flexure specimen for measuring mode II fracture toughness. Compos Sci Technol 1986;27(3):177–97. http://dx.doi.org/10.1016/0266-3538(86)90031-X.
[65] Davidson BD, Sun X. Effects of friction, geometry, and fixture compliance on the perceived toughness from three-and four-point bend end-notched flexure tests. J Reinf Plast Compos 2005;24:1611–28. http://dx.doi.org/10.1177/0731684405050402.
[66] Sun X, Davidson BD. Numerical evaluation of the effects of friction and geometric nonlinearities on the energy release rate in three- and four-point bend end-notched flexure tests. Eng Fract Mech 2006;73(10):1343–61. http://dx.doi.org/10.1016/j.engfracmech.2005.11.007.
[67] Davidson BD, Sun X, Vinciquerra AJ. Influences of friction, geometric nonlinearities, and fixture compliance on experimentally observed toughnesses from three and four-point bend end-notched flexure tests. J Compos Mater 2007;41:1177–96. http://dx.doi.org/10.1177/0021998306067304.